

Supporting Methods

Savas *et al.* 10.1073/pnas.0800658105

SI Text

Plasmids. To construct Flag-Htt590–25Q and Flag-Htt590–97Q, a DNA fragment encoding the first 574 residues of mouse Htt (NP_034544, equivalent in position to amino acid 596 in human Htt, NP_022102) was amplified by PCR using Htt-75 DNA as a template and subcloned into the mammalian expression vector pOZ-FH-N (1) digested with XhoI and NotI. A stop codon was introduced at the 3' end after the last Htt residue. The contiguous CAG repeat sequence was then replaced by a sequence containing a mixture of CAG and CAA codons encoding 25 or 97 glutamines (using plasmids obtained from Joan Steffan and Leslie Thompson, University of California, Irvine) to increase the stability of the repeat region. The resulting construct produced a fusion protein with N-terminal Flag and HA epitope tags fused to 670 N-terminal amino acids of Htt; first 59 residues of which contained the human sequence and the remaining contained the mouse sequence. Htt480–17Q and Myc-Htt590–25Q were gifts of Florian Then (Harvard Medical School, Boston). To construct Myc-Htt590ΔQ, DNA encoding 22 glutamines was deleted from Htt590–25Q. The Myc-Htt590–25QΔP construct was designed to lack residues 45 to 78 (NM_002111) but retained 25 glutamines.

Antibodies Used in Microscopy Experiments. Htt (Chemicon 2166, dilution: 1:250), Flag (Sigma, M2 monoclonal 1:100, polyclonal 1:100), Myc (Covance PRB-150C, 1:400), Ago2 (Upstate 07–590, 1:200), rabbit polyclonal Dcp1a [gift of J. Lykke-Andersen (University of Colorado, Boulder), 1:200], rabbit polyclonal HCF-1 (gift of A. Wilson, NYU School of Medicine, New York University 1:800), TIA-1 (Santa Cruz sc-1751, 1:100), rpS6 (Cell Signaling 2217, 1:500).

Purification of Flag-Htt590. Six liters ($\approx 4 \times 10^9$ cells) of Flag-Htt590 expressing HeLa S3 cells were harvested and lysed hypotonically followed by douncing (2). One gram of soluble S100 fraction in Buffer B (20 mM Hepes pH 7.6, 1.5 mM MgCl₂, 20% glycerol, 0.5 mM DTT, 0.5 mM PMSF, 0.5 mM sodium metabisulfite) + 150 mM KCl was incubated with 300 μ l of α -Flag M2 affinity resin (Sigma) for 3 h. The mixture was poured into a column and washed twice in Buffer B containing 350 mM KCl + 0.1 mM EDTA, and once in Buffer B + 150 mM KCl. Bound proteins were eluted at room temperature with the same buffer plus Flag peptide (300 μ g/ml). The proteins were concentrated in YM-10 spin columns (Amicon) before separation by 10% SDS NuPAGE (Invitrogen) and stained with SimplyBlue Coomassie (Invitrogen).

Mass Spectrometry. The gel lane was sectioned from top to bottom in 2-mm increments, and cut pieces placed in clean tubes. In-gel tryptic digestion was performed after two washes with 50% acetonitrile in 100 mM ammonium bicarbonate, and dehydration of gel slices with the addition of 100% acetonitrile. Disulfides were reduced with 45 mM DTT in 50 mM ammonium bicarbonate, and alkylated with 100 mM iodoacetamide in 50 mM ammonium bicarbonate. Gel pieces were again dehydrated with 100% acetonitrile. Trypsin (Promega) (260 ng/gel piece) was added and incubated overnight at room temperature. Peptides were extracted from the gel pieces by subsequent additions of 30% acetonitrile in 0.1% TFA and 80% acetonitrile in 0.1% TFA. Samples were dried, redissolved in 0.1% formic acid and injected into a Shimadzu HPLC system coupled to a Thermo Finnigan LCQ Classic. HPLC separation was performed on a

New Objectives Pico-frit column filled with BetaBasic C18. A linear gradient was developed from 10–60% B (A, 5% acetonitrile, 95% aqueous 0.1% formic acid; B, 80% acetonitrile, 20% aqueous 0.1% formic acid) at a rate of 1.5%/minute. Data were collected continuously for 60 min, selecting the 3 most intense ions (exceeding 3×10^6 intensity units) in a MS survey scan for subsequent MS/MS analyses using collisionally induced dissociation. Selected precursors were analyzed for 2 MS/MS cycles and then excluded for redundant analyses for a 90 sec interval. Thermo-Finnigan Excalibur 2.0 utility extract.msn was used to retrieve peak lists without any added smoothing or S/N criteria. The recorded MS/MS files were searched with the Mascot search engine 2.1.04 (Matrix Sciences) against the Swiss-Prot database (Sp_Trembl_122406.fas) with the limitation of mammalian species for protein database records; precursor ion mass tolerance 2.0; fragment-ion mass tolerance 0.8; methionine oxidation and carbamido methylation of cysteine allowed; trypsin specificity with one missed cleavage allowed.

Affinity Purification of Flag-Ago2. Flag-tagged Ago2 expressing construct and a selectable marker for puromycin resistance were cotransfected in HEK293T cells. Transfected cells were grown in presence of 5 μ g/ml puromycin (Sigma) for selection. Individual colonies were isolated and screened for Flag-tagged protein expression. Nuclear extracts of Flag-fusion-expressing cells (50 mg) were incubated with 250 μ l of Flag-M2 affinity resin (Sigma) for 2 h at 4°C. Beads were washed 4 times with 10 ml of BC500 buffer (20 mM Tris, pH 8, 0.5 M KCl, 10% glycerol, 1 mM EDTA, 1 mM DTT, 0.1% Nonidet P-40, 0.5 mM PMSF, aprotinin, leupeptide, and pepstatin, 1 μ g/ml each) and once with 10 ml BC100 buffer (20 mM Tris, pH 8, 0.1 M KCl, 10% glycerol, 1 mM EDTA, 1 mM DTT, 0.1% Nonidet P-40, aprotinin, leupeptin, and pepstatin, 1 μ g/ml each). Bound peptides were eluted with 400 μ g/ml Flag peptide (Sigma) in BC100 buffer.

Cell Extracts/Glycerol Gradient Sedimentation/Immunoprecipitations. For overexpression experiments, 1×10^6 HeLa cells were plated in 10-cm plates and transiently transfected 24 h later by using Lipofectamine 2000 (Invitrogen). Cell lysates were cleared by centrifugation at 12,000 RCF for 15 min and the soluble material transferred to a new tube. 1 mg of the S100 fraction was loaded onto 10–40% glycerol gradients and spun in a Beckman SW55 rotor at 43,000 rpm for 13 h as described (3). Immunoprecipitations were performed using 2.5 μ g of soluble α -Flag M2 (Sigma) antibody per reaction and collected with 25 μ l of 50/50 (vol/vol) Protein A and G beads (GE Healthcare). For immunoprecipitation of endogenous proteins, ten plates (10 cm) of HeLa cells were lysed in 3 ml (total volume) of TNEN buffer (10 mM Tris-HCl pH7.8, 150 mM NaCl, 1 mM EDTA, 1% Nonidet P-40) with protease inhibitors and sonicated (Branson Digital Sonifier) for 3 seconds at duty cycle of 25%. One mg of soluble protein was used per IP reaction with 3 μ g of antibody to Htt (Chemicon 2166) or mouse normal IgG (Santa Cruz Biotechnology), which was incubated overnight at 4°C. Thirty μ l of Protein A/G beads were added and samples incubated for 2 h and harvested by centrifugation. Washes were performed in HEMG buffer (25 mM Hepes-KOH pH7.9, 0.1 mM EDTA, 12.5 mM MgCl₂, 20% glycerol) containing 150 mM, 350 mM, or 500 mM KCl for 3 times followed by 1 wash with HEMG with 150 mM KCl. Proteins were eluted by boiling in 2X SDS loading buffer for 3 min before separation by SDS/PAGE.

Sequential siRNA Transfections. For microscopic analysis, U2OS cells were plated on glass cover slips in 60 mm plates at 4.5×10^4 cells per plate 24 h before siRNA transfection. For control HCF-1 siRNA experiments, 48 h after siRNA transfection, cells were fixed and permeabilized. For the sequential knockdown experiments, cells were first transfected with Luc siRNA or Htt siRNA and incubated for 48 h, after which cells were transfected with siRNA for HCF-1, and incubated for additional 48 h and analyzed as described above.

siRNA Sequence. (Sense strand, 5' to 3'): Luc, CUUACGCU-GAGUACUUCGA; Htt (mixture of 4), UAACGUGGCU-CAUUGUAAA, GAACUAUCCUCUGGACGUA, CAA-CAUGUGUGCAGUUACA, UAAUUAGGCUUGUCCC-AAA; HCF-1, GGAGCUCAUCGUGGUGUUU (4); TNRC6A (GW182), GAAUUGCUCUGGUCGCUA (5); Lamin A/C, CUGGACUCCAGAAGAACA; eIF6, CAAUU-GAAGACCAGGAUGA (6). siCONTROL Non-Targeting siRNA Pool #1 was from Dharmacon (D-001206-13). siAgo2-1 siRNA sequence was from (7). All siRNAs were purchased from Dharmacon.

Experiments with Mouse Striatal Cells. Immortalized striatal neuronal progenitor cells (8) expressing endogenous normal Htt (*STHdh*^{Q7/Q7}) or homozygous mutant Htt (*STHdh*^{Q111/Q111}) were split at 4×10^5 cells per 35 mm plate 24 h before transfection. Each plate was transfected with 200 ng SV40 promoter-Luc reporter, 50 ng CMV- β galactosidase, and 170 μ moles (8.5 μ l of 20 μ M) of Luc siRNA or siCONTROL siRNA (Dharmacon) mixed with 5 μ l of Lipofectamine 2000 (Invitrogen). Western blot analysis was performed by loading 75 μ g of RIPA lysate per lane and probing with indicated antibodies. Image analysis was performed on 100 cells from several cover slips and culture plates for *STHdh*^{Q7/Q7} and *STHdh*^{Q111/Q111} cells using NIH ImageJ software. Images were acquired with equal settings and the red channel was extracted as a tif file without contrast/brightness manipulation. The images were cropped to include only complete cells to facilitate accurate cell counts. The red channel was then converted to a black/white image (0–255) and thresholding was performed such that any intensity below 125 was discarded. Next, the image was watershed (default settings) and subsequently particle analysis was performed (default settings). The data from multiple images was combined and represented as the average number of P-bodies (particles) per cell counted.

FRAP. Fluorescence recovery after photobleaching was performed on a Zeiss LSM 510 Meta microscope with a 63x oil

immersion objective. The 488 nm laser line from a 30 mW argon laser was used for GFP-bleaching and the 458 nm line from the same laser was used for GFP-imaging. A 1mW 543 nm HeNe laser was used for both RFP-bleaching and -imaging. A Bioprotechs Delta T Controlled Culture Dish System (Bioprotechs) was used to maintain a stable cell environment during data acquisition. HeLa cells transfected with plasmids expressing EGFP-Ago2 (Addgene plasmid 11590) (5) and RFP-Dcp1a (gift of N. Kedersha, Harvard Medical School) were maintained in phenol-red free medium (OPTI-MEM, Invitrogen) during imaging. For bleaching, uniformly shaped, individual P-bodies, approximately equidistant from the plasma membrane and the nucleus, were chosen. A 2 μ m circle encompassing the P-body was bleached with a 300 ms pulse of both the bleaching lasers set at 100%. In general, this resulted in a bleach depth of between 30 and 70% for both fluorophores. Starting 3 second before and continuing 40 seconds after bleaching, fluorescence in both the red and green channel was recorded at 300 ms intervals. An area of $\approx 24 \times 48 \mu$ m around the bleached spot was imaged with the imaging lasers set at 25% (458 nm) and 20% (543 nm), respectively. The data were normalized to the prebleach intensity of each bleach spot and corrected for loss of signal during image acquisition, as described (9, 10). For convenience, we assumed a reaction-dominant binding reaction, and an unbiased value for the recovery fraction (C_{eq}) and k_{off} for each experiment was estimated by fitting the normalized recovery fraction to an inverse exponential decay function [$f(t) = C_{eq} * (1 - e^{-k_{off}t})$; (11)]. To avoid bias for the slow recovery phase, every 5 time points between 10–40 seconds post bleach were averaged before fitting to the model (11). Between 7 and 10 individual cells were assayed for each condition. Curve fitting was done with Labfit line fitting software.

It is our understanding that decrease in recovery fraction (% recovery) is an accepted measurement in FRAP experiments (12, 13) and interestingly, was also observed in the published study on Ago2 dynamics (14). Further, we purposefully chose a conservative level of bleaching (50–70% reduction) in anticipation of problems that might arise from inconsistency in bleach depth. This necessitates compensating for remnant fluorescence as outlined by (9, 10). In addition, we assessed changes in gross binding site competency for the recovering population in each bleached area using a “double bleach” approach (9). After the first bleach and recovery, each spot was immediately re-bleached and the second recovery recorded. After compensating for the specific bleach depth in each segment, we found no significant variation in the recovery rate for each bleaching cycle. The significance of the reduced recovery by GFP-Ago2 is underscored by the fact that this does not occur with RFP-Dcp1a even though the two fluorophores were bleached simultaneously.

1. Nakatani Y, Ogryzko V (2003) Immunoaffinity purification of mammalian protein complexes. *Methods Enzymol* 370:430–444.
2. Dignam JD, Lebovitz RM, Roeder RG (1983) Accurate transcription initiation by RNA polymerase II in a soluble extract from isolated mammalian nuclei. *Nucleic Acids Res* 11:1475–1489.
3. Tanese N (1997) Small-scale density gradient sedimentation to separate and analyze multiprotein complexes. *Methods* 12:224–234.
4. Julien E, Herr W (2003) Proteolytic processing is necessary to separate and ensure proper cell growth and cytokinesis functions of HCF-1. *EMBO J* 22:2360–2369.
5. Jakymiw A, et al. (2005) Disruption of GW bodies impairs mammalian RNA interference. *Nat Cell Biol* 7:1267–1274.
6. Chendrimada TP, et al. (2007) MicroRNA silencing through RISC recruitment of eIF6. *Nature* 447:823–828.
7. Meister G, et al. (2004) Human Argonaute2 mediates RNA cleavage targeted by miRNAs and siRNAs. *Mol Cell* 15:185–197.
8. Trettel F, et al. (2000) Dominant phenotypes produced by the HD mutation in *STHdh*(Q111) striatal cells. *Hum Mol Genet* 9:2799–2809.
9. Stavreva DA, McNally JG (2004) Fluorescence recovery after photobleaching (FRAP) methods for visualizing protein dynamics in living mammalian cell nuclei. *Methods Enzymol* 375:443–455.
10. Phair RD, Gorski SA, Misteli T (2004) Measurement of dynamic protein binding to chromatin in vivo, using photobleaching microscopy. *Methods Enzymol* 375:393–414.
11. Sprague BL, Pego RL, Stavreva DA, McNally JG (2004) Analysis of binding reactions by fluorescence recovery after photobleaching *Biophys J* 86:3473–3495.
12. McNally JG (2008) Quantitative FRAP in analysis of molecular binding dynamics in vivo *Methods Cell Biol* 85:329–351.
13. Stavreva DA, McNally JG (2006) Role of H1 phosphorylation in rapid GR exchange and function at the MMTV promoter. *Histochem Cell Biol* 125:83–89.
14. Leung AK, Calabrese JM, Sharp PA (2006) Quantitative analysis of Argonaute protein reveals microRNA-dependent localization to stress granules. *Proc Natl Acad Sci USA* 103:18125–18130.

A.

# peptides	Htt590	Ago1	Ago2
Flag-590-25Q	17	7	14
Flag-590-97Q	18	0	2

B.

Htt590-25Q	Argonaute Isoform(s)
Argonaute peptide	
R.VLPAPILQYGGR.N	1
R.SVSIPAPAYYAR.L	1
R.QEIIEDLSYMVR.E	1
K.NTYSGLQLIIVILPGK.T	1,3
K.IDVYHYEVDIKPDK.C	1
R.VGDTLLGMATQCVQVK.N	1,3,4
K.AQPVIEFMCEVLDIR.N	1
K.NASYNLDPYIQEFGIK.V	1
R.DGVPEGQLPQILHYELLAIR.D	1
R.ELLIQFYK.S	1,2,3,4
R.VLQPPSILYGGR.N	2
K.VWAIACFAPQR.Q	2
K.NLYTAMPLPIGR.D	2
R.QEIIQDLAAMVR.E	2
K.AIATPVQGVWDMR.N	2
K.LQANFFEMDIPK.I	2
K.DYQPGITFIVVQK.R	2
R.DAGMPIQGQPCFCK.Y	1,2,3,4
K.MMLNIDVSATAFYK.A	1,2,3
K.NTYAGLQLVVILPGK.T	2
R.YPHLPCLQVQGEQK.H	1,2,3,4
R.VGDTVLMATQCVQMK.N	2
K.IDIYHYELDIKPEK.R	2
K.AQPVIEFVCEVLDK.S	2
R.SVSIPAPAYYAHVAFR.A	2,3
K.HTYLPLEVCNIVAGQR.C	1,2,3,4
R.LPSVPFETIQALDVVMR.H	2
R.DGVSEGQFQQVLHHELLAIR.E	2
R.FSSDELQILTYQLCHTYVR.C	2

Htt590-97Q	Argonaute Isoform(s)
Argonaute peptide	
R.DAGMPIQGQPCFCK.Y	1,2,3,4
R.VLQPPSILYGGR.N	2
K.AQPVIEFVCEVLDK.S	2
R.VGDTLLGMATQCVQVK.N	1,3,4
R.DAGMPIQGQPCFCK.Y	1,2,3,4
K.HTYLPLEVCNIVAGQR.C	1,2,3,4

Fig. S1. (A) Tabulated peptide counts (number of peptides identified) from a representative Htt purification. Distinct peptides corresponding to Htt590, Ago1 and Ago2 with Mascot scores greater than 15 are included in the table. A similar trend in peptide counts was observed in two independent Htt purifications. (B) Tabulated tryptic peptides identified by ESI-Ion trap MS/MS corresponding to the Ago isoforms with Mascot scores greater than 15. Peptide searches were performed using the Sp_Trembl database (taxonomy = mammalian), fixed modification = carbamidomethyl(C), variable modification = oxidation(M), mass values = monoisotopic, peptide mass tolerance ± 1.5 Da, fragment mass tolerance ± 0.8 Da, and 1 allowed missed tryptic cleavage. Distinct Ago peptides are indicated by a single assignment in the isoform field and peptides shared by multiple Agos are indicated accordingly.

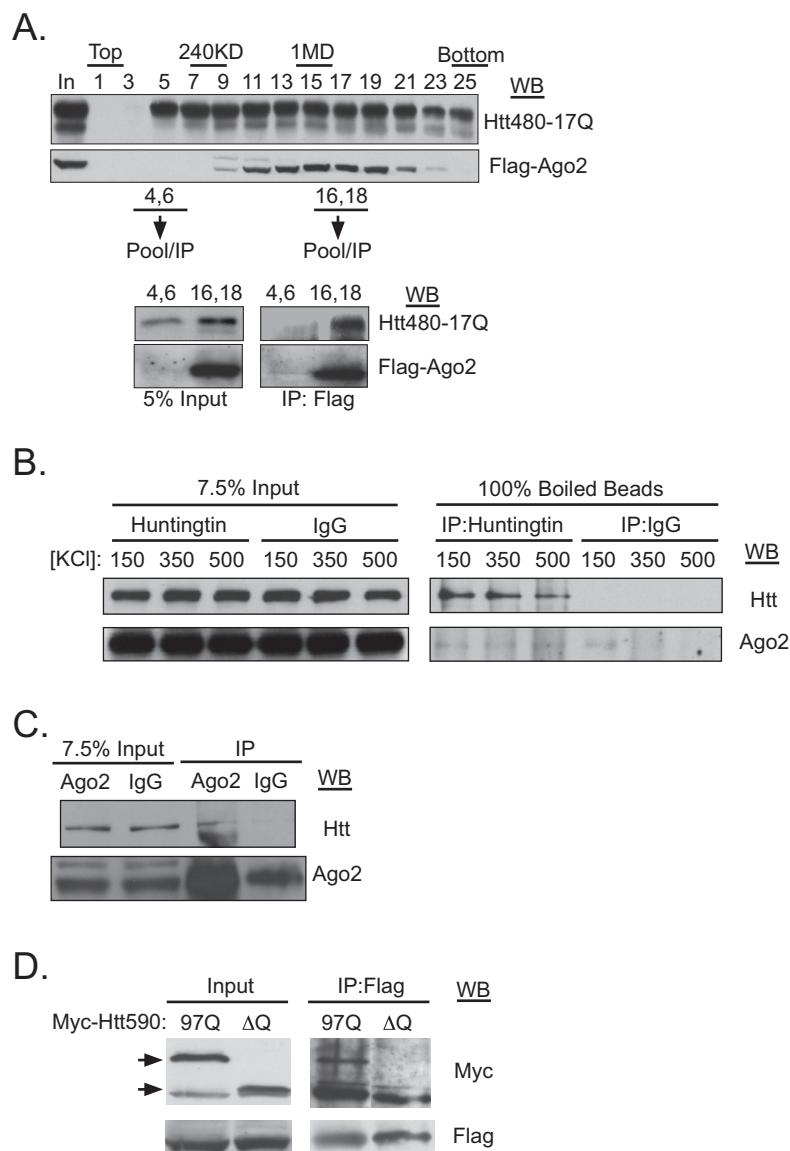


Fig. S2. Huntingtin associates with Ago2. (A) S100 fraction from HeLa cells cotransfected with Flag-Ago2 and Htt480-17Q was fractionated by sedimentation on a 10–40% glycerol gradient. Approximate sedimentation positions of proteins of known molecular mass are shown above the gradient. Odd numbered fractions were TCA precipitated and analyzed by immunoblotting. The indicated even fractions were pooled, immunoprecipitated with α -Flag antibody and analyzed. (B) HeLa cell lysate was immunoprecipitated with an antibody to Htt or control IgG and probed for endogenous Ago2. Endogenous Htt and Ago2 co-precipitated in the presence of 350 mM and 500 mM KCl. (C) HeLa cell lysate was immunoprecipitated with an antibody to Ago2 or control IgG and probed for endogenous Htt. (D) HeLa cells were cotransfected with Myc-Htt590-97Q or Δ Q, and Flag-Ago2. Ago2 was immunoprecipitated with α -Flag antibody and the presence of Htt was determined by immunoblotting with α -Myc antibody. Arrows point to Myc-Htt590-97Q and Myc-Htt590- Δ Q.

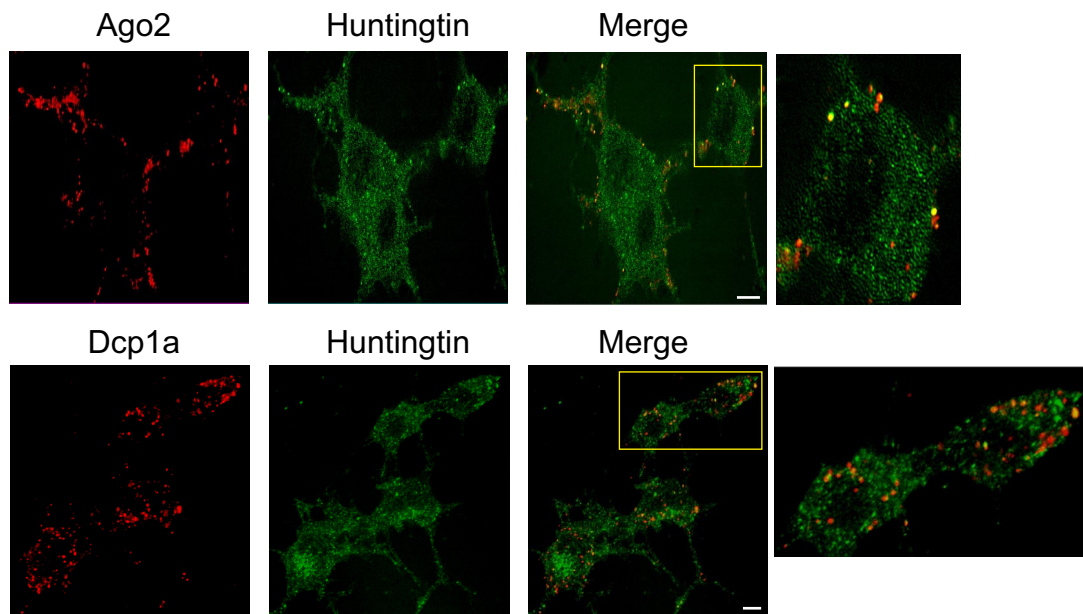


Fig. S3. Mouse neuronal N2A cells were probed for endogenous Ago2 and Dcp1a with rabbit polyclonal antibodies. Htt was localized with a mouse monoclonal antibody. The secondary antibodies used were goat α -rabbit Alexa 488 and goat α -mouse Alexa 555 conjugated antibodies (bar = 20 μ m). Of 50 cells examined, 45% of foci showed Ago2 and Htt co-localization. Of 50 cells examined, 55% of foci showed Dcp1a and Htt co-localization.

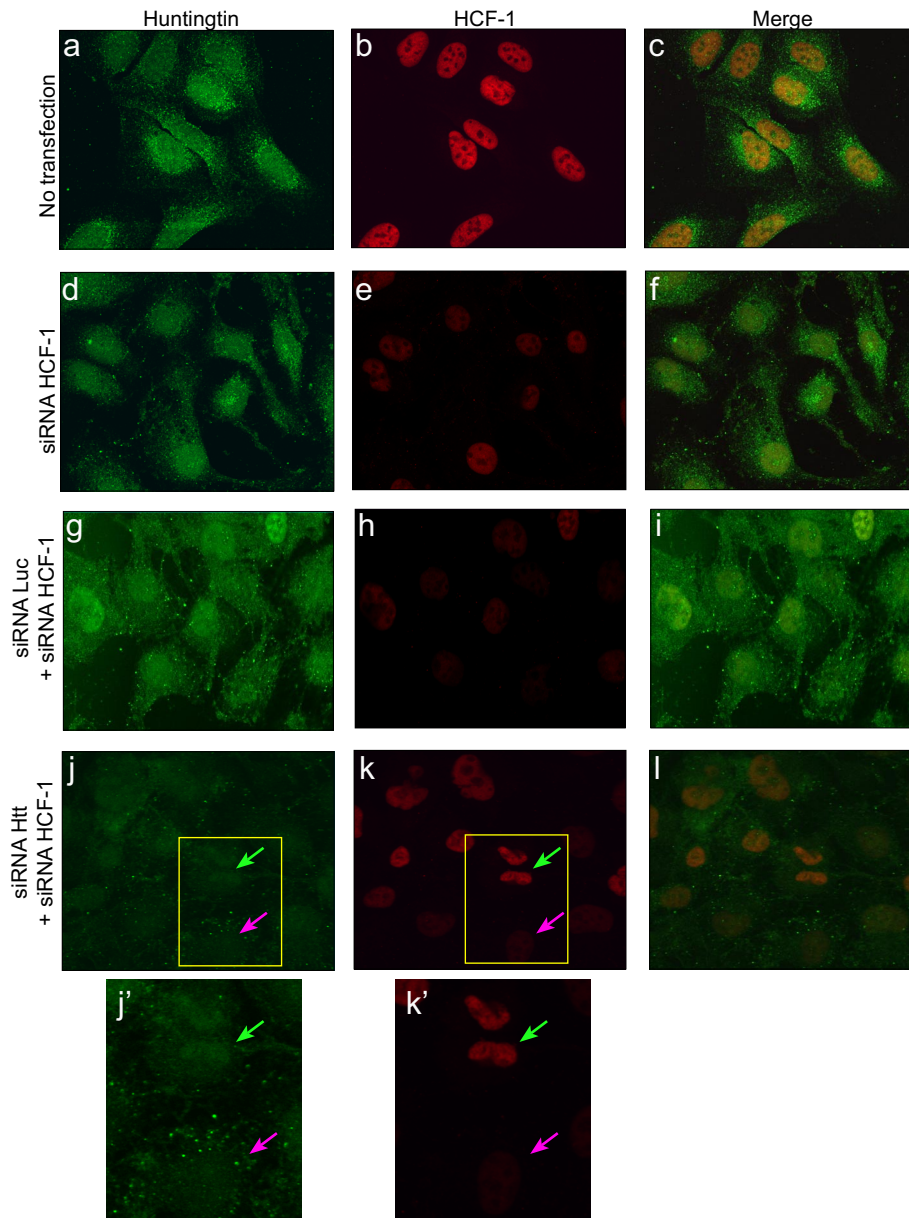


Fig. S4. The effect of Htt knockdown on the ability to silence HCF-1 was assessed by indirect immunofluorescence. Untransfected (*a-c*) or HCF-1 siRNA-transfected (*d-f*) U2OS cells were probed as described in [SI Text](#) with α -Htt and α -HCF-1 antibodies. Additional cells were first transfected with Htt siRNA (*j-l*) or Luc siRNA (*g-i*) and incubated for 48 h. HCF-1 siRNA was then transfected and cells were incubated for an additional 48 h. Depletion of HCF-1 protein was efficient as seen from comparison of the equivalent fluorescent intensity by indirect immunofluorescence to that of untransfected cells (compare *b* and *e*). Cells transfected with Htt siRNA (*j-l*) were examined for the relative HCF-1 signal. Cells with reduced Htt puncta (*j'* and *k'*, green arrow) consistently demonstrated compromised ability to silence HCF-1 when compared with adjacent cells that possessed higher Htt puncta and reduced HCF-1 staining (*j'* and *k'*, pink arrow), suggesting a role for Htt in siRNA-induced silencing of HCF-1.

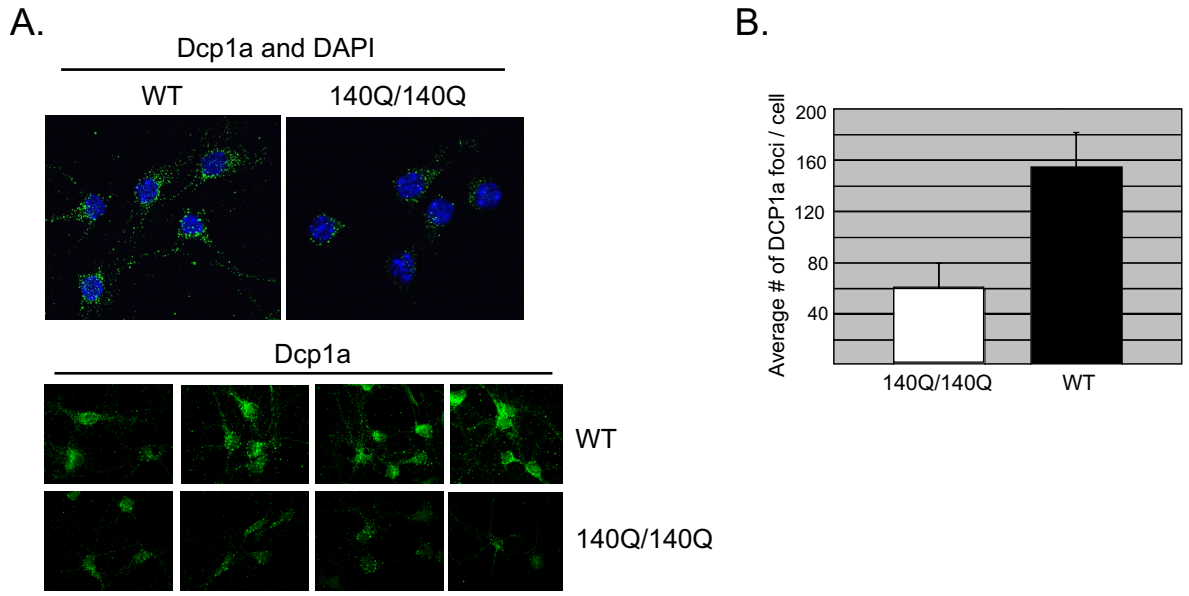


Fig. S5. (A) Primary neurons from wt or mutant HD mice (*Hdh^{Q140/Q140}*) were stained with α -Dcp1a antibody and DAPI. Representative images are shown. (B) Quantification of the number of Dcp1a foci per cell. ($n = 28$, 140Q/140Q; $n = 26$, WT).

Table S1. FRAP measurements

	Mock		Htt590–25Q		Htt590–97Q	
	C_{eq}	k_{off}	C_{eq}	k_{off}	C_{eq}	k_{off}
Ago2	0.141 +/-0.054	0.402 +/-0.280	0.147 +/-0.049	0.293 +/-0.118	0.091 +/-0.028*	0.285 +/-0.414
Dcp1a	0.250 +/-0.044	0.367 +/-0.370	0.287 +/-0.122	0.194 +/-0.074	0.220 +/-0.089	0.285 +/-0.194

The recovery of fluorescence of either fluorescent protein was assumed to be diffusion-uncoupled and thus the recovery fraction (C_{eq}) and the k_{off} rate for the average recovery curve was determined by fitting the data against an inverse exponential recovery function describing a reaction dominant recovery [$f(t) = C_{eq} * (1 - e^{-k_{off}t})$]. The error is given as the 95% confidence interval for the fitted data of 7–10 individual P-bodies for each condition. * $P > 0.05$, relative to the mock transfection.